ELSEVIER

Chemical promotional effect of gold added to palladium supported on cerium oxide in catalytic methanol decomposition

Mahendra P. Kapoor [a,1], Yuichi Ichihashi [a,2], Toshie Nakamori [b], Yasuyuki Matsumura [b,*]

[a] *National Institute of Advanced Industrial Science and Technology, Midorigaoka, Ikeda,Osaka 563-8577, Japan*
[b] *Research Institute of Innovative Technology for the Earth, Chemical Research Group, 9-2 Kizugawadai, Kizu-cho, Soraku-gun, Kyoto 619-0292, Japan*

Abstract

Addition of gold to palladium by simultaneous deposition–precipitation on cerium oxide increases the catalytic activity for methanol decomposition to carbon monoxide and hydrogen at 180 °C. No significant promotional effect was observed by addition of rhodium or iridium to palladium. The electronic state or dispersion of palladium is unchanged by the addition of gold, suggesting presence of new active sites. Bimetallic clusters of Pd–Au can be formed by the addition of gold, but an excessive amount of gold results in formation of fairly large gold particles on the support. The increase in the activity does not relate to the number of the gold particles and addition of a small quantity of gold significantly promotes the reaction, suggesting that the bimetallic clusters are highly active in the methanol decomposition.
© 2004 Elsevier B.V. All rights reserved.

1. Introduction

Methanol decomposition to carbon monoxide and hydrogen has recently attracted a growing interest because the endothermic reaction is applicable to the energy recovery of the waste heat from a methanol-fuelled automobile and industries [1,2], while new catalysts being active at low temperatures below 200 °C are required especially in the application to industries. Palladium is active to the reaction especially when the support is cerium oxide on which palladium is cationic [3–7]. It is known that modification of palladium with gold often results in improvement in the catalytic activity of palladium for reactions such as hydrogenation, oxidation, decomposition etc. [8–12]. In the reactions formation of Pd–Au alloy is probably indispensable for the promotional effect of gold which is basically inactive metal [8,12,13]. Hence, the preparation process of

homogeneous alloy is important especially for supported catalysts while the preparation accompanies difficulty [14]. For example, Lam and Boudart showed a successful formation of Pd–Au clusters on silica by ion-exchange with $[Au(en)_2]^{3+}$ and $[Pd(NH_3)_4]^{2+}$ [13,15], but impregnation with the metal chlorides did not produce well-homogenized bimetallic clusters [16]. In the present paper, we will show formation of the bimetallic clusters on cerium oxide by a deposition–precipitation method and significant increase in the catalytic activity of palladium supported on cerium oxide for methanol decomposition by addition of gold, while the preparation technique is applicable to other supports.

2. Experimental

Palladium and/or gold was supported on cerium oxide (Daiichi Kigenso Kogyo, $98 \, m^2 \, g^{-1}$) by the deposition–precipitation method described elsewhere [6]. Palladium and/or gold hydroxides were exclusively precipitated on the oxide in a $PdCl_2$ (Kanto Kagaku, GR grade) and/or $AuHCl_4$ (Kanto, GR) aqueous solution by gradual addition of $1 M \, Na_2CO_3$ (Kanto, GR) solution. The solid was dried at 120 °C overnight and calcined in air at 300 °C for 3 h. The samples contained 5 wt.% of palladium and 0.1–5 wt.%

of gold (n wt.% Au–Pd/CeO$_2$ where n represents the gold content). Preparation of 2 wt.% Rh–Pd/CeO$_2$ or Ir–Pd/CeO$_2$ was carried out by the same procedure as described above, except addition of RhCl$_3$ (Kanto, GR) or H$_2$IrCl$_6$ (Kanto, GR) instead of AuHCl$_4$.

Catalytic reaction was performed in a fixed-bed continuous flow reactor under atmospheric pressure. A catalyst (0.20 g) diluted with 1.0 g of quartz sand being inert under the reaction conditions was sandwiched with quartz wool plugs in a quartz tube reactor of 6 mm i.d. The samples were reduced in a flow of 20 vol.% hydrogen diluted with argon (flow rate, 9.6 dm^3 h^{-1}) for 1 h at 300 °C, then 20 vol.% of methanol was fed with an argon carrier (total flow rate 4.8 dm^3 h^{-1}) at 180 °C. The outlet gas was analyzed with an on-stream gas chromatograph (Yanagimoto G2800) equipped with a Porapak-T column (4 m) and a thermal conductivity detector.

X-ray photoelectron spectra (XPS) were recorded at room temperature with a Shimadzu ESCA 3200. After reduced with hydrogen (0.02 MPa) at 300 °C for 1 h in a vacuum line, the sample was mounted in air to a sample holder. In order to remove surface adsorbates, Ar-ion sputtering for 0.5 min at 2 kV and 20 mA was carried out just before the measurement. It was confirmed that the spectra after the sputtering are very similar to those of the samples reduced in situ [6,17]. Binding energies were corrected by the reference of the C 1s line at 284.6 eV. The surface molar ratios of Au/Pd, Pd/Ce, and O/Ce were calculated from the peak areas using the atomic sensitivity factors of Au 4f (4.95), Pd 3d (4.6), Ce 3d (10), and O 1s (0.66) [18].

Profiles of extended X-ray absorption fine structure (EXAFS) for the samples were taken at room temperature in transmission mode for Pd K-edge and in fluorescence mode for Au L$_3$-edge at beam-line BL01B1 of SPring-8. The samples were reduced with hydrogen (0.02 MPa) at 300 °C for 1 h in a vacuum line and sealed with polyethylene films in nitrogen atmosphere. The Fourier transformation was performed on k^3-weighted EXAFS oscillations in the range of 30–150 nm^{-1}. Inverse Fourier transform of Pd K-edge was obtained within the windows 0.18–0.28 nm in r space. The Pd–Pd reference was derived from the EXAFS of Pd foil. The analysis was performed with a program of "REX" supplied by Rigaku.

Powder X-ray diffraction (XRD) patterns of the reduced samples were recorded with a Rigaku RINT 2000 diffractometer using nickel-filtered Cu Kα radiation.

Transmission electron microscopy (TEM) observations were made using Hitachi H-9000.

3. Results and discussion

3.1. Catalytic activity of metal-modified Pd/CeO$_2$

Gold-modified palladium supported on cerium oxide effectively catalyzed the selective methanol decomposition to
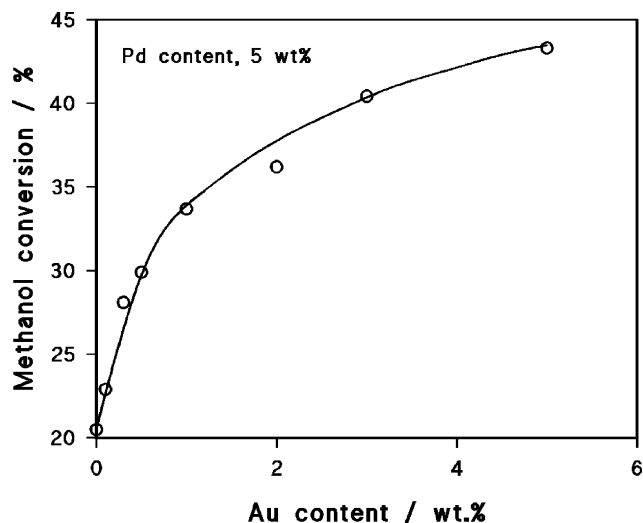

Fig. 1. Catalytic activity of Au-modified Pd/CeO$_2$ in the methanol decomposition to carbon monoxide and hydrogen at 180 °C.

hydrogen and carbon monoxide at 180 °C. The activity of the catalyst increased with an increase in the content of gold, and addition of 3 wt.% of gold doubled the conversion of 20.5% produced with gold-free Pd/CeO$_2$ (Fig. 1).

Although rhodium and iridium are generally active metal in comparison with gold, the promotional effect was very small, that is, the methanol conversions were 22.6 and 21.6% (selectivity to carbon monoxide, 100%) with 2 wt.% Rh–Pd/CeO$_2$ and Ir–Pd/CeO$_2$. Since ceria-supported gold (3 wt.%) catalyst prepared by the deposition–precipitation method was inactive under the reaction conditions, palladium is essential in the catalysis and gold probably assists the function.

3.2. Electronic state of Pd and Au in catalyst

In order to understand the promotional effect of gold, the surface characterization by XPS was performed on some typical samples of Au–Pd/CeO$_2$. The activity of palladium for the decomposition relates to the electronic state detectable by XPS [3–7,19]. The binding energy of Pd 3d$_{5/2}$ for ceria-supported palladium free from gold (Pd/CeO$_2$) was 355.8 eV (Fig. 2). The energy of palladium metal is 335.0 eV [18], showing that the palladium species in the samples are cationic and activated by the interaction with the support [3,6]. The binding energy of Pd 3d$_{5/2}$ for PdO is 336.3 eV [18] and Kili et al. reported that the peak at 336.8 ± 1 eV is attributed to PdO in Pd/γ-Al$_2$O$_3$ modified with cerium or lanthanum oxide [20]. Since the valence of palladium generally relate to the binding energy [18], the valence of the major palladium species in the samples is probably close to +1. Although the activity of Au–Pd/CeO$_2$ is higher than that of Pd/CeO$_2$, the addition of gold does not change the binding energy of Pd 3d$_{5/2}$ significantly (Table 1). No significant change in the surface molar ratio of Pd/Ce was observed by addition of gold to Pd/CeO$_2$
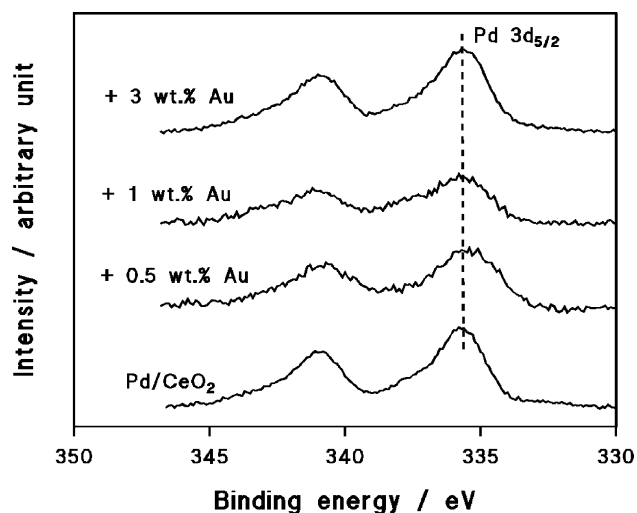
Fig. 2. XPS of Pd 3d region for Au-modified Pd/CeO$_2$ reduced at 300 °C.

Table 1
XPS parameters of Au-modified Pd/CeO$_2$ reduced at 300 °C

Sample	Binding energy (eV)				Surface atomic ratio		
	Pd 3d$_{5/2}$	Au 4f$_{7/2}$	Ce 3d$_{5/2}$	O 1s	Au/ Pd	Pd/ Ce	O/ Ce
Pd/CeO$_2$	335.7	–	882.5	529.6	0.0	0.09	2.7
0.5 wt.% Au–Pd/CeO$_2$	335.5	83.6	882.5	529.8	0.05	0.09	2.8
1 wt.% Au–Pd/CeO$_2$	335.6	83.6	882.4	529.6	0.06	0.07	3.0
3 wt.% Au–Pd/CeO$_2$	335.6	83.8	882.5	529.7	0.26	0.10	2.7

(see Table 1). Thus, the modification of gold does not change the electronic state or surface concentration of palladium significantly. The binding energies of Au 4f$_{7/2}$ in Au–Pd/CeO$_2$ was 83.6–83.8 eV (Fig. 3 and Table 1), which is almost the same as that of metallic gold [17], showing no significant electronic interaction between palladium and gold.
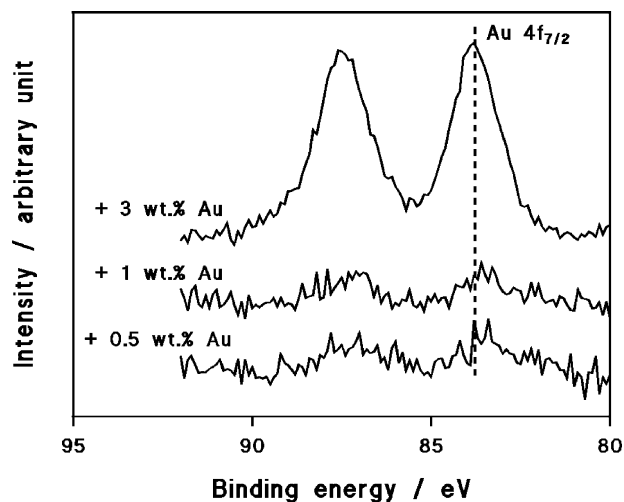

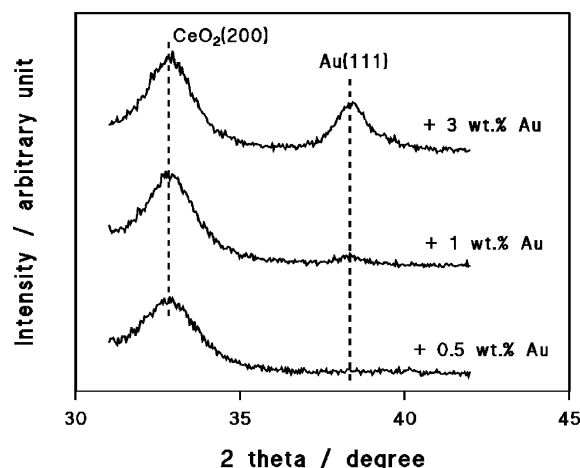Fig. 3. XPS of Au 4f region for Au-modified Pd/CeO$_2$ reduced at 300 °C.

Fig. 4. XRD patterns of Au-modified Pd/CeO$_2$ reduced at 300 °C.

3.3. Structural analyses by XRD and TEM

Peaks at 38.4° in 2θ attributed to Au [1 1 1] were confirmed in the XRD patterns of 1 and 3 wt.% Au–Pd/CeO$_2$, while no such peak was observed with 0.5 wt.% Au–Pd/CeO$_2$ (Fig. 4). The mean crystallite sizes of the gold particles in 1 and 3 wt.% Au–Pd/CeO$_2$ were estimated as 9 and 8 nm, respectively, from the line broadening [21]. No peaks attributed to palladium were recorded in the patterns of Pd/CeO$_2$ and Au–Pd/CeO$_2$, showing absence of Pd particles whose size is larger than 3 nm.

No particles attributed to palladium or palladium–gold were detected in the TEM pictures of Pd/CeO$_2$ and Au–Pd/CeO$_2$, but fairly large gold particles were present on the surface of 1 and 3 wt.% Au–Pd/CeO$_2$. The mean particle size of gold on 1 wt.% Au–Pd/CeO$_2$ was 15.3 nm (20 particles from 4.5 to 26.2 nm) and that on 3 wt.% Au–Pd/CeO$_2$ was 13.3 nm (18 particles from 8.3 to 21.2 nm) (Fig. 5). Since the two samples show similar particle size
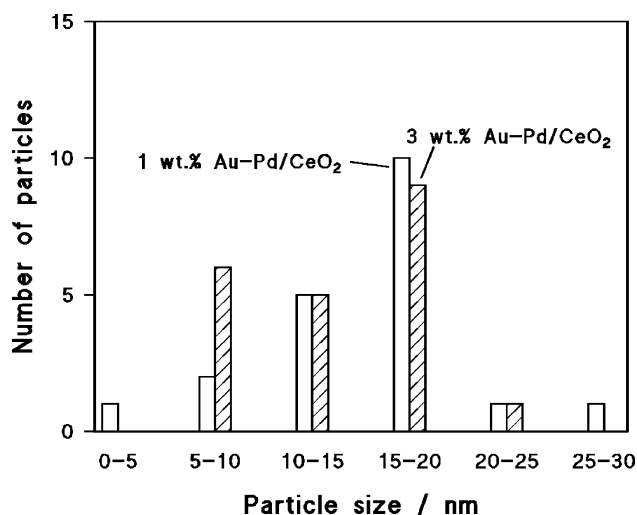

Fig. 5. Particle size distribution of gold on Au-modified Pd/CeO$_2$ observed by TEM.
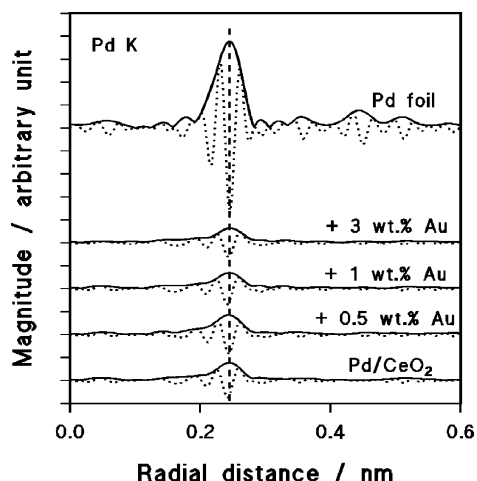
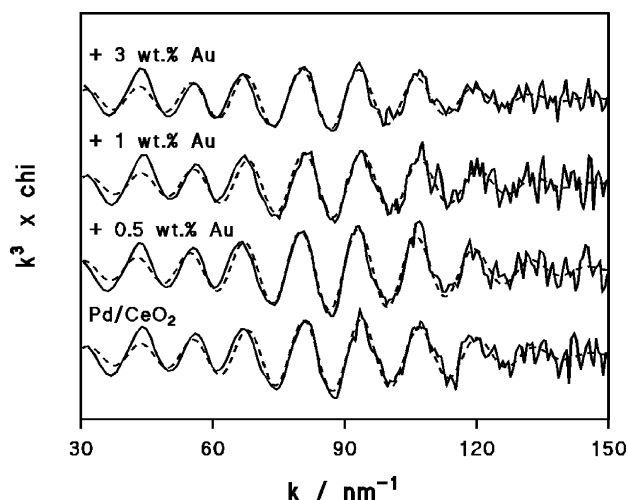Fig. 6. Fourier transforms of k^3-weighted Pd K-edge EXAFS for Au-modified Pd/CeO$_2$ reduced at 300 °C.

Fig. 7. k^3-Weighted Pd K-edge EXAFS oscillations for Au-modified Pd/CeO$_2$ reduced at 300 °C. Solid line, experimental data; broken line, calculated fit.

distribution, the number of the gold particles should relate to the XRD peak intensity, but that for 1 wt.% Au–Pd/CeO$_2$ was significantly weaker than expected from the gold content. Hence, the fairly large gold particles are a minor part of gold in 1 wt.% Au–Pd/CeO$_2$ and the major part is undetectable by XRD. The large gold particles detected in XRD and TEM are probably inactive or less active, because the increase in the catalytic activity by addition of gold does not relate to the XRD peak intensity.

3.4. Structural analyses by EXAFS

In order to analyze the atomic structure of palladium and gold, EXAFS (extended X-ray absorption fine structure) analyses were performed. The Fourier transforms of the Pd K-edge EXAFS for the gold-modified samples reduced at 300 °C for 1 h showed presence of weak peaks at 0.24 nm (phase shift uncorrected) mainly attributed to Pd–Pd interaction, and they were very similar to that of the unmodified one (Fig. 6). The coordination numbers of the first Pd–Pd shell for Au–Pd/CeO$_2$ were determined as 5.3–5.6 by curve-fitting and almost the same as that for Pd/CeO$_2$ (Table 2 and Fig. 7). The first shell fitting was carried out

ignoring the contribution of the higher shells because the magnitude of the peaks attributed to the shells were very weak (see Fig. 6) [22]. The small coordination numbers show the dispersion of palladium or palladium–gold particles on the gold-modified samples is similar to that on the unmodified one. Thus, addition of gold to Pd/CeO$_2$ does not affect the dispersion of palladium, and it is in harmony with the XPS result in Table 1. The mean particle sizes can be estimated as ca. 1 nm from the coordination numbers of 5.3–5.6 by the standard method proposed by Greegor and Lytle assuming spherical particle [23]. The shorter bond distances than in Pd foil suggest the stronger Pd–Pd interaction because of the lower coordination number.

The Fourier-transform of the Au L$_3$-edge EXAFS for 0.5 wt.% Au–Pd/CeO$_2$ was significantly different from that for Au foil (Fig. 8). Although the curve-fitting to determine

Table 2
EXAFS parameters of Pd–Pd interaction for Au-modified Pd/CeO$_2$ reduced at 300 °C

Sample	Interatomic distance, R (nm)	Coordination number, N	Debye–Waller factor, σ (nm)	ΔE_0 [a] (eV)
Pd foil	0.275	12.0	0.0060	0.0
Pd/CeO$_2$	0.271	5.4	0.0091	1.0
0.5 wt.% Au–Pd/CeO$_2$	0.272	5.5	0.0087	−2.0
1 wt.% Au–Pd/CeO$_2$	0.271	5.3	0.0093	1.0
3 wt.% Au–Pd/CeO$_2$	0.272	5.6	0.0098	0.1

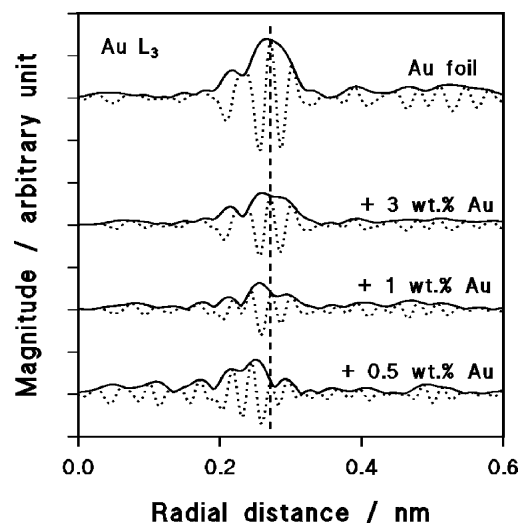[a] Difference in the ionization threshold energy between reference and sample.

Fig. 8. Fourier transforms of k^3-weighted Au L$_3$-edge EXAFS of Au-modified Pd/CeO$_2$ reduced at 300 °C.

the bonding parameters was difficult because of the noises in the spectra, the peak position in the profile (0.25 nm, phase shift uncorrected) is apparently smaller than that for Au–Au interaction in Au foil (0.27 nm), showing presence of bonding shorter than Au–Au in Au foil. Since the bond length in gold metal is 0.288 nm and the distance of Au–Pd was reported to be 0.278 ± 0.001 nm in Pd–Au bimetallic clusters on silica [11,13], the shorter distance can be mainly attributed to Pd–Au interaction. Thus, gold atoms are probably dispersed in the palladium particles in 0.5 wt.% Au–Pd/CeO$_2$ and presence of gold clusters on the surface is denied. In the case of 3 wt.% Au–Pd/CeO$_2$, the peak position was similar to that for Au foil, showing presence of gold particles and it is in consistent with the observations by TEM and XRD. Although presence of gold particles was observed on 1 wt.% Au–Pd/CeO$_2$, the Fourier-transform is dissimilar to that of 3 wt.% Au–Pd/CeO$_2$ and somehow close to that of 0.5 wt.% Au–Pd/CeO$_2$. This strongly suggests coexistence of Au–Pd and Au–Au interactions, and the Au–Au interaction is mainly due to the presence of gold particles detected by XRD (see Fig. 4). The presence of Au–Pd interaction shows that gold atoms are also dispersed in the palladium particles in 1 wt.% Au–Pd/CeO$_2$, and one can suppose that a part of gold in 1 wt.% Au–Pd/CeO$_2$ is excluded from the nano-size Pd–Au clusters and forms the large gold particles.

3.5. The activity of Pd–Au clusters

In the case of 3 wt.% Au–Pd/CeO$_2$, a large part of gold may be excluded from the nano-size Pd–Au clusters and forms the large gold particles detected by XRD (see Fig. 4). However, the concentration of gold in the Pd–Au clusters should be increased with increase in the gold content, while it will be gradually saturated at the higher concentrations. Since the catalytic activity is highly promoted by addition of a small quantity of gold and gradually saturated by addition of a larger amount of gold (see Fig. 1), it is estimated that gold atoms or clusters in the Pd particles are promote the activity of palladium.

The XPS analyses show no change in the electronic state of palladium or gold, suggesting that the activity of palladium or gold itself does not improved. Hence, it is rather considered that gold atoms assist the catalytic function of palladium. On the basis of kinetic studies, the rate determining step of the methanol decomposition over palladium is estimated to be the interaction between methoxyl groups and surface hydrogen formed by dissociative adsorption of methanol [24,25], that is, CH$_3$O–Pd+H–Pd $\rightarrow$ CH$_2$O–Pd+ H$_2$ + Pd. It is known that adsorption strength of carbon monoxide or molecular hydrogen on gold is weak [26], but gold in palladium–gold foil can interact with atomic hydrogen [27]. Thus, a step, CH$_3$O–Pd + Au $\rightarrow$ CH$_2$O–Pd + H–Au, may contribute to the reaction, while further elucidation is necessary to clarify it.

References

[1] National Research Council, Catalysis Look to the Future, National Academy Press, Washington, DC, 1992.
[2] T. Nishimura, T. Omata, Y. Ogisu (Eds.), Eco-Energy City System (in Japanese), Energy Conservation Center, Tokyo, 1999.
[3] Y. Usami, K. Kagawa, M. Kawazoe, Y. Matsumura, H. Sakurai, M. Haruta, Appl. Catal. A 171 (1988) 123.
[4] Y. Usami, K. Kagawa, M. Kawazoe, Y. Matsumura, H. Sakurai, M. Haruta, Stud. Surf. Sci. Catal. 118 (1998) 83.
[5] Y. Matsumura, Y. Ichihashi, Y. Morisawa, M. Okumura, M. Haruta, Stud. Surf. Sci. Catal. 130 (2000) 2315.
[6] W.-J. Shen, Y. Matsumura, Phys. Chem. Chem. Phys. 2 (2000) 1519.
[7] W.-J. Shen, Y. Matsumura, J. Mol. Catal. A 153 (2000) 165.
[8] E.G. Allison, G.C. Bond, Catal. Rev. 7 (1972) 233.
[9] S.H. Inami, H. Wise, J. Catal. 26 (1972) 92.
[10] C.J. Baddeley, M. Tikhov, C. Hardacre, J.R. Lomas, R.M. Lambert, J. Phys. Chem. 100 (1996) 2189.
[11] S.N. Reifsnyder, H.H. Lamb, J. Phys. Chem. B 103 (1999) 321.
[12] A. Malinowski, W. Juszezyk, J. Pielaszek, M. Bonarowska, M. Wojeieehowska, Z. Karpiński, Stud. Sur. Sci. Catal. 130 (2000) 1991.
[13] R.J. Davis, M. Boudart, J. Phys. Chem. 98 (1994) 5471.
[14] G.C. Bond, Chem. Soc. Rev. 20 (1991) 441.
[15] Y.L. Lam, M. Boudart, J. Catal. 50 (1977) 530.
[16] M. Bonarowska, J. Pielaszek, W. Juszczyk, Z. Karpiński, J. Catal. 195 (2000) 304.
[17] W.-J. Shen, Y. Ichihashi, M. Okumura, Y. Matsumura, Catal. Lett. 64 (2000) 23.
[18] D. Briggs, M.P. Seah (Eds.), Practical Surface Analysis (Second Edition) Vol. 1: Auger and X-ray Photoelectron Spectroscopy, John Wiley & Sons, Inc., New York, 1990.
[19] Y. Matsumura, M. Okumura, Y. Usami, K. Kagawa, H. Yamashita, M. Anpo, M. Haruta, Catal. Lett. 44 (1997) 189.
[20] K. Kili, L. Hilaire, F. Le Normand, Phys. Chem. Chem. Phys. 1 (1999) 1623.
[21] H.P. Klug, L.E. Alexander, X-ray Diffraction Procedures, Wiley, New York, 1954.
[22] M.P. Kapoor, Y. Ichihashi, W.-J. Shen, Y. Matsumura, Catal. Lett. 76 (2001) 139.
[23] R.B. Greegor, F.W. Lytle, J. Catal. 63 (1980) 476.
[24] N. Fukuhara, S. Sekiguchi, H. Mutoh, T. Igarashi, Kagaku Kogaku Ronbunshu 21 (1995) 1002.
[25] S. Shiizaki, I. Nagashima, Y. Matsumura, M. Haruta, Catal. Lett. 56 (1998) 227.
[26] M. Haruta, Catal. Today 36 (1997) 153.
[27] P.G. Dickens, J.W. Linnett, W. Palczewska, J. Catal. 4 (1965) 140.